SCIENCE CHINA
Information Sciences

• **Supplementary File** •

Multi-Path Navigation Method Using Solar Panel-Reflected Solar Oscillations for Earth Satellites

Yang Yuqing[1], Yang Haonan[1], Ning Xiaolin[1*], Wu Weiren[2] & Fang Jiancheng[1]

[1]*School of Instrument Science & Opto-electronics Engineering, Beihang University, Beijing*100191*, P.R.China ;*
[2]*Lunar Exploration and Space Program Center, China National Space Administration, Beijing* 100037*, P.R.China*

Appendix A The constraints of Earth occlusion and reflected angle

During the measurement acquisition process, three Earth occlusion cases need to be considered: (1) the line of the Earth satellite to the Sun is blocked; (2) the line of the reflected satellite to the Sun is blocked; (3) the line of the Earth satellite to the reflected satellite is blocked. To ensure that the direct and reflected solar oscillations can pass through the Earth occlusion, the position of the Earth satellite and reflected satellite should satisfy the constraints as follows:

$$\begin{cases} acos(\dfrac{\boldsymbol{r}_{ps} \cdot \boldsymbol{r}_{ep}}{|\boldsymbol{r}_{ps}||\boldsymbol{r}_{ep}|}) > asin(\dfrac{R_e}{|\boldsymbol{r}_{ep}|}) \\ acos(\dfrac{\boldsymbol{r}_{rs} \cdot \boldsymbol{r}_{er}}{|\boldsymbol{r}_{rs}||\boldsymbol{r}_{er}|}) > asin(\dfrac{R_e}{|\boldsymbol{r}_{er}|}) \\ acos(\dfrac{\boldsymbol{r}_{er} \cdot \boldsymbol{r}_{ep}}{|\boldsymbol{r}_{er}||\boldsymbol{r}_{ep}|}) > acos(\dfrac{R_e}{|\boldsymbol{r}_{er}|}) + acos(\dfrac{R_e}{|\boldsymbol{r}_{ep}|}) \end{cases} \tag{A1}$$

where $\boldsymbol{r}_{ps}$ is the position vector of the Earth satellite to the Sun; $\boldsymbol{r}_{es}$, $\boldsymbol{r}_{ep}$, and $\boldsymbol{r}_{er}$ are the position vectors of the Sun, Earth satellite, and reflected satellite to the Earth, respectively; R_e is the Earth's radius = 6378.137 km; and $\boldsymbol{r}_{rs}$ is the position vector of the reflected satellite to the Sun.

Since the solar panel is generally installed towards the Sun to collect more energy, the solar panel always tries to keep pointing to the Sun. To obtain the solar panel reflected solar oscillations, the constraints of the reflected angle should be satisfied. To simplify the analysis, we assume that the normal of the solar panel is collinear with $\boldsymbol{r}_{rs}$. Thus, the judgment of the reflected angle can be written as Eq.(A2) to ensure that the reflected solar oscillations can be obtained by the satellite.

$$acos(\frac{\boldsymbol{r}_{rp} \cdot \boldsymbol{r}_{rs}}{|\boldsymbol{r}_{rp}||\boldsymbol{r}_{rs}|}) > \alpha \tag{A2}$$

where α is the threshold of the reflected angle and it is set as 45° in this paper.

Appendix B The simulation conditions

The trajectory of the Earth satellite, the reflected satellite, and the Sun is produced by the System Tool Kit (STK). The propagator of the Earth satellite is High Precision Orbit Propagator (HPOP) and its orbit parameters can be shown as follows: semi-major-axis: 7263.77km; eccentricity: 0.002407; inclination: 98.867°; argument of perigee: 92.631°; RAAN: 29.253°; true Anomaly: 118.274°. The propagator of BeiDou M3-1 ∼ BeiDou M3-24 satellite is SGP4, and the ideal orbit of the GPS satellite is generated by the STK constellation database.

The simulation period was from UTCG 31 May 2022 04:00:00.000 to 30 Jun 2022 04:00:00.000. The filter period is set as 3s. The initial position and velocity errors are set as [1000m;1000m;1000m] and [0.1m/s;0.1m/s;0.1m/s], respectively. The measurement noise is considered as random error, and the standard deviation of the measurement error as 10ns. Aims at exploring the achievable navigation accuracy, the ephemeris errors of Sun, Moon, and reflected satellites are not considered in this paper.

Appendix C Navigation performance of the reflected solar oscillations

The performances of FY-1 using Moon-reflected solar oscillations and solar panel-reflected solar oscillations are shown in Figure C1 and Figure C2, respectively. In Figure C2, the value of measurement availability "1" represents visible and "0" represent invisible. The influence of the measurement error of time delay on the newly proposed method is shown in Table C1.

* Corresponding author (email: celenavbuaa@sina.cn)

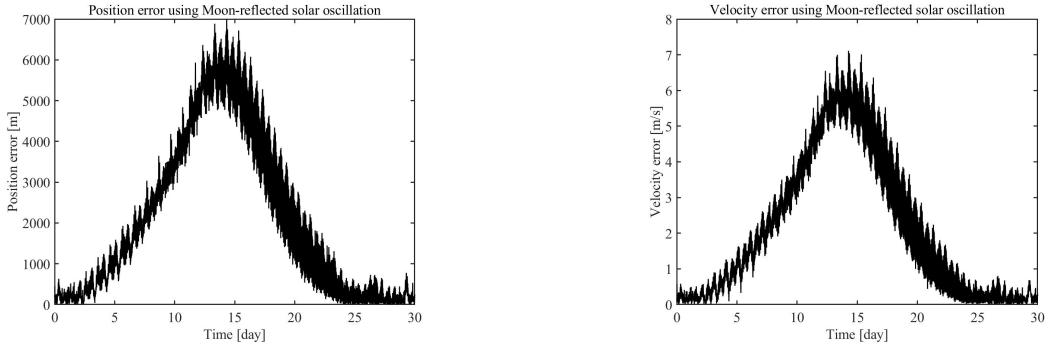

Figure C1 Navigation performance of FY-1 using Moon-reflected solar oscillation. (a) Position error; (b) Velocity error

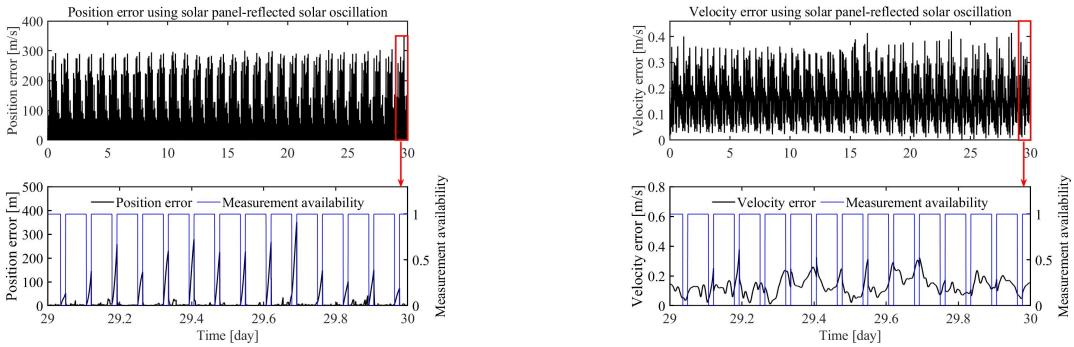

Figure C2 Navigation performance of FY-1 using solar panel-reflected solar oscillations. (a) Position error; (b) Velocity error

Table C1 The influence of the measurement error of time delay on the newly proposed method

Measurement noise[s]	Mean error		Maximum error	
	Position error[m]	Velocity error[m/s]	Position error[m]	Velocity error[m/s]
10^{-9}	17.51	0.13	305.55	0.40
10^{-8}	20.61	0.13	351.44	0.42
10^{-7}	33.84	0.12	482.24	0.58
10^{-6}	72.03	0.10	580.32	0.61
10^{-5}	295.96	0.29	1448.1	1.25